Available online at www.sciencedirect.com
SCIENCE DIRECT®
ELSEVIER
Nuclear Instruments and Methods in Physics Research A 553 (2005) 187–195
NUCLEAR INSTRUMENTS & METHODS IN PHYSICS RESEARCH Section A
www.elsevier.com/locate/nima

Results from the ageing studies of large CsI photocathodes exposed to ionizing radiation in a gaseous RICH detector

A. Braem[a], G. De Cataldo[a,b], M. Davenport[a], A. Di Mauro[a], A. Franco[b], A. Gallas[a], H. Hoedlmoser[a], P. Martinengo[a], E. Nappi[b], F. Piuz[a,*], E. Schyns[a]

[a]*CERN, Geneva, Switzerland*
[b]*INFN-Sez. di Bari, Bari, Italy*

Available online 12 September 2005

Abstract

We studied the ageing of large CsI photocathodes induced by ionizing particles (^{90}Sr) by correlating the integrated charge dose of the ionic avalanches hitting the photocathode to the local changes of the Quantum Efficiency (QE). The drop of the QE of the irradiated CsI spots is reported as a function of the charge dose. It was found that the ageing process continues even in absence of irradiation.

Keywords: MWPC; CsI; RICH; Cherenkov; Ageing; Photocathode; ALICE; LHC

1. Introduction

CsI photocathodes (CsI-PC) of large area are currently used as photoconverters in RICH systems based on gaseous photo-detectors [1–5]. Several mechanisms are known to contribute to the ageing of CsI-PCs, resulting into a degradation of the quantum efficiency (QE). First, owing to the strong affinity of CsI to water, extended presence of moisture is responsible for a permanent chemical damage. The QE degradation resulting from a short exposure to air ($\leqslant$hour) can be recovered by heating the PC in vacuum at about 60 °C [6]. Accordingly, in order to prevent and minimize such a damage, the insertion of all our PCs in the detector is performed under constant flow of an inert gas, thus keeping continuously the fraction of water (and oxygen) in the containing vessels below the 10 ppm level.

Illumination by an intense photon flux ($\geqslant 10^{12}\,\mathrm{cm}^{-2}$, s^{-1}) also damages the CsI-PC [7]. However, such an intensity is not achieved in common RICH applications as a consequence of the low yield of Cherenkov photons, therefore, this effect will not be considered in this article. This work deals with the damage induced by the exposure to ionizing radiation. In this case the

*Corresponding author. Tel.: +41 79 776 6580.
E-mail address: francois.piuz@cern.ch (F. Piuz).

0168-9002/$ - see front matter © 2005 Elsevier B.V. All rights reserved.
doi:10.1016/j.nima.2005.08.059

QE degradation is caused by the ions produced in the gaseous avalanches, which bombard the resistive layer of CsI deposited onto the cathode of the wire chamber. During the R&D phase, tests were usually carried out on small PCs prototypes [8]. At that time, not much care was taken to avoid exposing the irradiated CsI-PC samples to air. Moreover, the measurements were performed using intense photon flux thus providing quite different evaluations of the induced damages. The goal of our test was to single out the role played by the charged particle radiation in the QE degradation of the photocathodes developed for the ALICE–HMPID modules. The correlation between the integrated ionic charge per unit area and the resulting CsI-QE drop was compared to the charge dose expected in an operation period of 10 years of the ALICE experiment.

2. Ageing experiment

2.1. Irradiation set-up and the ionic charge measurement

A new detector based on the HMPID design [9] but of smaller size so as to be equipped with only one full size CsI-PC ($64 \times 40\,cm^2$) was built. For the purpose of our study, the detector was equipped with an array of three collimated ^{90}Sr sources and one small C_6F_{14} radiator of 50 mm diameter, located at a distance of 100 mm from the pad plane as shown in Fig. 1. With this geometry, the Cherenkov photons produced by the beam particles filled a circular fiducial region of 148 mm mean radius. The analysis of the ring pattern provided a measurement of the photon energy dependence of the CsI-QE [9]. As shown in Fig. 1, the axis of each radioactive source intersected orthogonally the cathode plane around the mean Cherenkov circle (Fig. 1a).

The collimator distance to the cathode pad plane was chosen so that the region of maximum irradiation density covered an array of 4×5 pads (pad size $8.0 \times 8.4\,mm^2$). This area was in turn overlapped by the Cherenkov fiducial zone allowing to compare the CsI-QE of irradiated spots with the remaining region. Moreover, at each spot, 20 pads of the irradiated zones were connected together in order to measure the integrated charge dose given by the cathode current generated during the irradiation.

In addition to the measurement of the anodic and cathodic currents, every pad signal was recorded by the FEE (based on the GASSIPLEX analog multiplexed read-out [10]) using the anode signals as a trigger.

The spots were irradiated using ^{90}Sr sources either of 29.9 or 260 MBq activity (see Table 1). At each position, only the 8 anode wires overlapping the 4×5 pads array were raised at the working amplification voltage, the rest of the anode plane being kept at 400 V, restricting in this way the effect due to the irradiation only to a strip of $33.6 \times 640\,mm^2$. The currents of the 8 wires (I_{8anod}) and of the 20 pads (I_{20pads}) were recorded using a CAEN-N671A[1] and a Keithley 617,[2] respectively. The proportionality of the amplification regime was checked up to the maximum voltage used of 2167 V. The currents were found perfectly stable up to 8 days of continuous irradiation, indicating that no anodic ageing was induced. Besides the mentioned irradiation tests, short runs were taken at lower rates to measure the charge pad profile as shown in Fig. 2. The ionic charge densities, Q_{int} (cm^{-2}), integrated during the irradiations can be derived at the 4×5 pads area from the values of I_{20pads} and the pad charge profile. This was the maximum density since the multiple scattering was responsible for the broad charge distribution, which extended significantly outside the 4×5 pads area along the anode wires. It was checked that the same densities could be derived from the anodic currents. The measurements relative to 4 irradiations are shown in Table 1.

2.2. Local measurement of the CsI-QE

During the CsI evaporation, the quantum efficieny is measured pad-by-pad using a VUV-scanner as described in Ref. [11]. Varying the position of a collimated VUV beam (D_2-lamp)

[1]CAEN SpA, 55049 Viareggio, Italy.
[2]Keithley Instr. Inc. Cleveland, 44139 Ohio, USA.

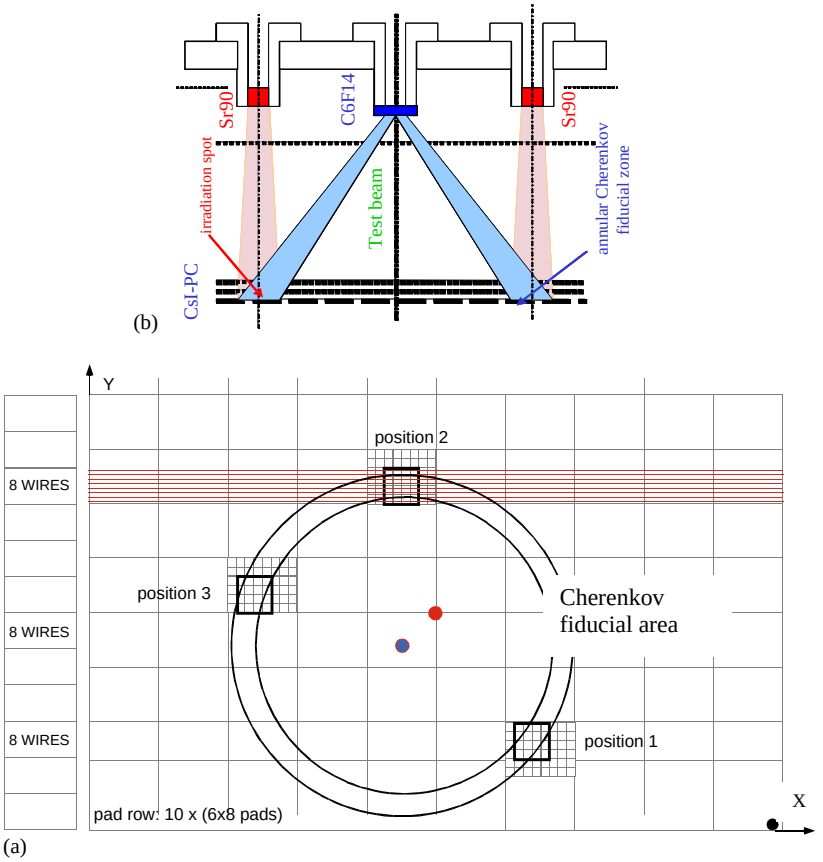

Fig. 1. (a) Locations of the three irradiation spots. The anode wires are horizontal (X-coordinate). The Cherenkov annular zone overlaps the three spots; (b) cross-section of the detector along a plane containing the centres of the radiator and spots 1 and 3. The RICH has a proximity focusing geometry, with an electrode collecting the ionization deposited along the proximity gap. The MWPC has a 2 mm half gap, 4.2 mm anode pitch. The pad size is $8.0 \times 8.4\,mm^2$, all coated with CsI. The chamber gas is CH_4. Each ^{90}Sr source is embedded in a plexiglas cylinder and collimated by a 10 mm long hole, 4 mm diameter, closed by a 50 μm thick mylar foil.

Table 1
Main data of the irradiation runs. The fourth spot was obtained by rotating the PC, 180°, clockwise

Position	Source (MBq)	Duration (hr)	8anod HV (V)	I_{8anod} (nA)	I_{20pads} (nA)	Q_{int} (mC/cm^2)	Dose rate (mC/cm^2,h)
1	29.9	196.3	2167	661	121	6.4	0.033
2	260	192.85	1980	563	132	6.8	0.051
3	260	48	1965	543	122	1.57	0.033
4	29.9	100	2050	158	36	0.5	0.01

with 5 mm spot diameter, the photocurrents are sequentially measured at every pad. They are referred as I_{norm} after being normalized to a reference PM (Hamamatsu R972).[3] The same apparatus was used to measure the PCs after irradiation. The mean photocurrent outside the irradiated spots, $\langle I_{ref} \rangle$, was also recorded. A variation of $\pm 2\%$ was observed over 6 months. The QE-drop will be expressed as an inefficiency, defined as $(I_{ref}-I_{norm})/I_{ref}$. Then, the PC

[3]Hamamatsu Photonics SARL, 91300 Massy, France.

was periodically scanned to study the time evolution of the QE in absence of irradiation (see Section 3.2).

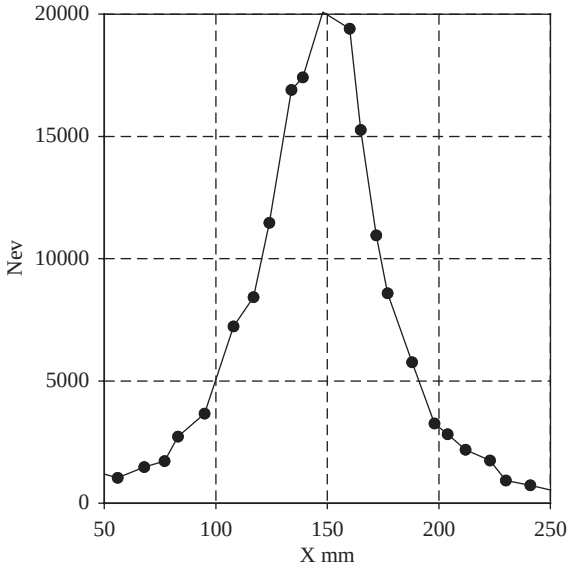

Fig. 2. Ionic charge profiles: along the X-coordinate obtained from the distribution of the charge centroids of the pad clusters.

3. Results

3.1. Measurements of the QE-drop and dependence on the charge dose

The pad photocurrent as obtained from the scan of the entire PC is shown in Fig. 3, the three spots irradiated at different doses are clearly visible. The attempt to recover the initial QE value by heat treatment was unsuccessful [11]. As shown in Fig. 4, the steep edges of the distribution of the pad photocurrent across the wires reflect the fact that the irradiated area is delimited in the Y direction by the 8 anode wires set at full voltage. On the contrary, the pad-photocurrent distribution along the wires (X direction) reflects the broad charge profiles as already shown in Fig. 2.

After the second irradiations, the detector was exposed to a 120 GeV/c π-beam. Fig. 5 shows the fiducial area filled with the Cherenkov photons produced in the C_6F_{14} 10 mm thick radiator. The low photoelectron yield in correspondence of the three irradiated spots clearly indicates the local degradation of the QE. The QE-curves obtained

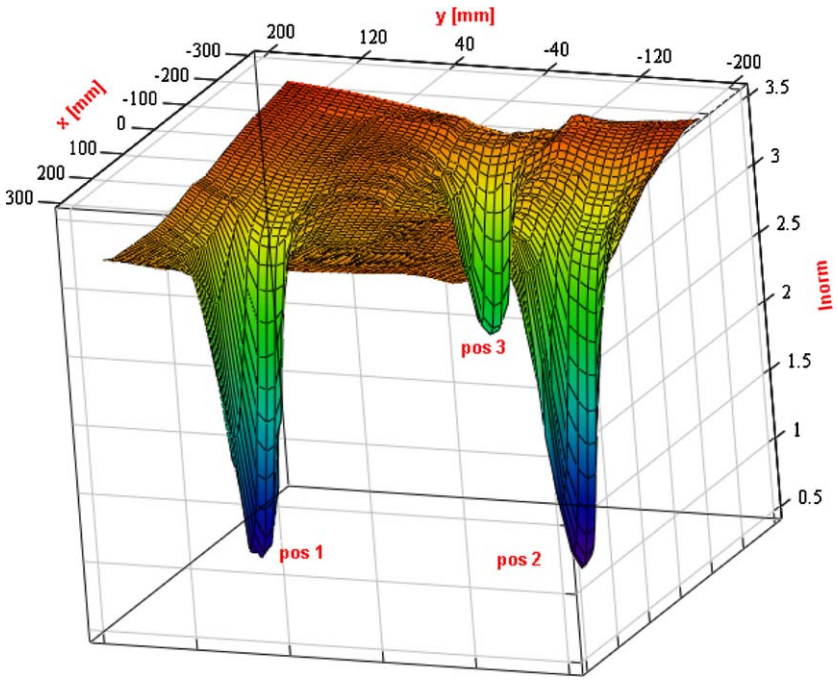

Fig. 3. Photocurrent of the entire PC is shown in the 3D-plot with the three spots irradiated at different doses.

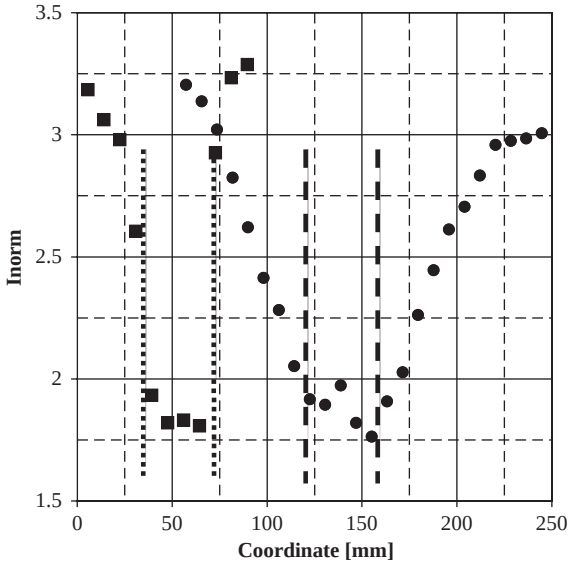

Fig. 4. Pad photocurrents, Inorm plotted vs. X and Y coordinates. The dotted lines indicate the size of the direct irradiation cone: 4×5 pads in X (dots) and the 8 anodes wires raised to full voltage in Y (square).

by the analysis of the Cherenkov rings reproduce the inefficiency profiles measured with the VUV-scanner.

Having recorded the charges and the photocurrents at identical X–Y steps, the aim was to evaluate the dependence of the QE-drop on the ionic charge along the pad row or column. However, before doing so, we report on the occurrence of an unexpected phenomenon.

3.2. Time evolution of the QE in absence of irradiation: post-ageing

Position 2 was the first spot being irradiated and the PC was scanned 5 days after the irradiation. Subsequently, in order to minimize the number of transfers of the PC to the VUV-scanner, it was decided to scan again the three spots 40 days after irradiation of positions 1 and 3. Although in this second exposure, position 2 was not irradiated, a further QE-drop was observed also in this position. This drop was not attributable to an overall degradation of the PC since the O_2 and H_2O fractions were monitored and found always below 10 ppm. Moreover, the QE measured outside the irradiated spots was found stable. After this operation, the PC was no more irradiated or set under voltage but it was scanned several times over a period of 280 days to study the long term evolution. As shown in Fig. 6, a continuous decrease of the QE was observed at the 3 positions finally followed by a partial QE recovery. The same degradation was observed in positions 1 and 2, having received the same integrated doses. It was checked that the degradation does not extend with time to non-irradiated area.

4. Discussion

4.1. Tentative modeling of the ageing mechanism

The approach is based on simple phenomenological aspects of the charge neutralization at the CsI surface.

In a first step, the aim is to estimate the fraction of ion impacts that kills a CsI photoemissive site. Let assume that the Nsite/mm^2 of the CsI surface are all efficient according to the characteristic QE curve. This density equals 5×10^{12} (mm^{-2}) according to the CsI lattice constant $= 4.56$ Å. Then it is assumed that every ion, which hits the PC kills the corresponding site, resulting in setting the QE to 0 and in neutralizing the ion charge. This is clearly an "extreme" hypothesis, not presupposing for the time being any detailed atomic mechanism. Such a mechanism, taking place at the CsI surface, might be driven by a cesiation reaction [12], although this mechanism is contested in Ref. [13].

An irradiation run is characterized by the ionic charge Q_{int} (mC/mm^2) integrated over the duration of the run, N_{sec} (s). The number of ions per avalanche, N_{ion}, is obtained from the chamber gain and the number of primary electrons created in the chamber gap. The mean rate of event is given by:

$$R(\text{s}^{-1}, \text{mm}^{-2}) = (Q_{\text{int}})/(e \times N_{\text{ion}} \times N_{\text{sec}})$$

where e is the electron charge, $e = 1.6 \times 10^{-19}$ C.

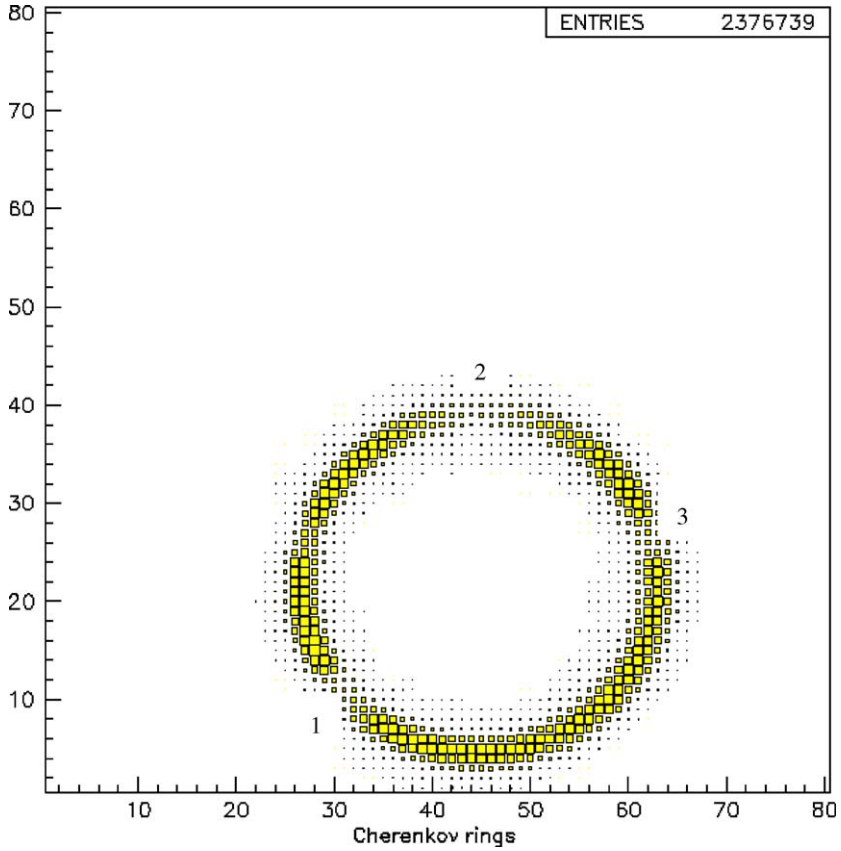

Fig. 5. Accumulated Cherenkov rings overlapping the 3 irradiated spots.

The fraction of sites hit by ions, equivalent to the occupancy, is given by (1)

$$\mathrm{OCC}(\mathrm{s}^{-1},\mathrm{mm}^{-2}) = (N_{\mathrm{ion}}/N_{\mathrm{site}}) \times R = (Q_{\mathrm{int}})/(e \times N_{\mathrm{site}} \times N_{\mathrm{sec}}). \quad (1)$$

Under the present assumption, since every ion kills a site, the above relation expresses the QE inefficiency, INEFF (s^{-1}, mm^{-2}). During the irradiation time t, the ions will more and more hit sites already dead and the variation with time of the inefficiency can be derived as

$$\mathrm{INEFF}(\mathrm{s}^{-1},\mathrm{mm}^{-2}) = 1 - \exp(-t \times \mathrm{OCC}). \quad (2)$$

Let us consider the first run in position 2, which was VUV-scanned immediately after irradiation. The following quantities were measured: Q_{int} after 193 h was equal to $6\,\mathrm{mC/cm^2}$ at a gain of 2×10^4, i.e. $N_{\mathrm{ion}} \approx 1 \times 10^5$ at the CsI-PC. The inefficiency was 42% and the irradiation rate was $5.2\,\mathrm{kHz/mm^2}$.

Introducing these values in Eq. (2), an inefficiency of 100% is reached in a time much smaller than N_{sec}. In order to fit the measured inefficiency, one might assume that each ion impact has a probability P_{ineff} to kill a photoemissive site. P_{ineff} should be taken as 1×10^{-2} for the irradiation at position 2. This value also provides a good fit for the irradiation in position 4 where $Q_{\mathrm{int}} = 0.5\,\mathrm{mC/cm^2}$, $N_{\mathrm{sec}} = 3.6 \times 10^5\,\mathrm{s}$, VUV-scan just after irradiation and ineff = 8%.

In a second step, we address the question whether the remaining charge (99%) be neutralized by leakage current through the CsI layer, assuming in addition that such a mechanism keeps the CsI-sites efficient.

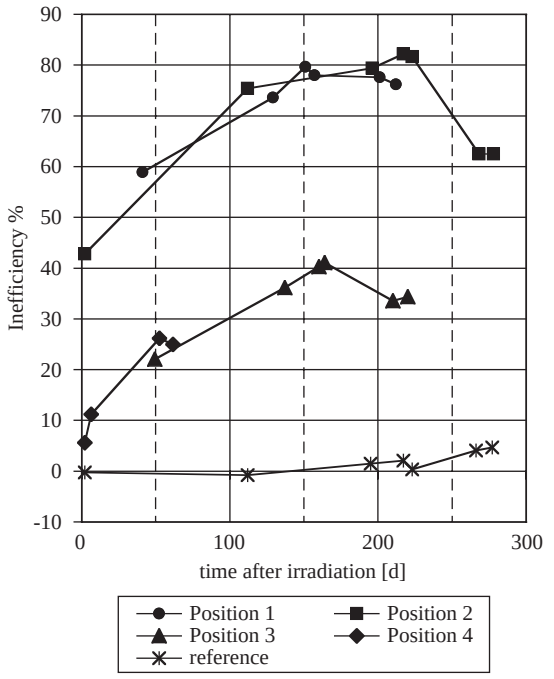

Fig. 6. Increase with time of the inefficiency in absence of irradiation at the four irradiation spots. The variation of $\langle I_{\mathrm{ref}} \rangle$ is indicated.

The ions impinging and stuck at a cathode coated with a resistive layer build up a voltage drop at the surface, $\Delta V = Q/C$ where Q is the ionic charge and C the capacitance of the layer per surface unit. The consequences are two-fold. At some level of charge build up, the electrical field through the layer can reach a breakdown limit causing usually a disruption of the detector (Malter effect [14]). Also, the chamber gain will be seen to decrease.

With $Q\ (\mathrm{mm}^{-2},\ \mathrm{s}^{-1}) = e \times \mathrm{Nsite} \times \mathrm{OCC}$ and $\varepsilon_0 = 8.87 \times 10^{-12}$, $\varepsilon_r = 4$, $S = 1\,\mathrm{mm}^2$, $d = 300\,\mathrm{nm}$, one gets a voltage drop of $\Delta V(V) = 6750 \times \mathrm{OCC}$.

It can be seen that the more stringent limitation of ΔV is given by the field strength. Assuming a breakdown limit of 30 kV/cm, ΔV must be kept less than 0.9 V, that is OCC $< 1.4 \times 10^{-4}$. Such a voltage drop is not expected to affect the gain.

Let us consider now the leakage current through the CsI layer. The current leakage time constant T_0 is $\varepsilon_0 \varepsilon_r \rho$. Taking a safety factor of 10 and a CsI bulk resistivity of $\rho = 2.8 \times 10^{10}\,\Omega\,\mathrm{cm}$ [15], one can express the ion occupancy as $\mathrm{OCC} = (10 \times T_0 \times R)/N_{\mathrm{site}}$, equal to 1×10^{-4}. This value is smaller than the previous limitation making the charge neutralization by leakage possible. In such a regime, the leakage current neutralizes the incoming ions as one goes along, leaving at the surface a stable amount of charge corresponding to the occupation value calculated above without initiating neither a breakdown nor a gain variation. At all the rates operated during the irradiations, we stress the fact that the amplification regime was found proportional up to the maximum voltage, the currents were constant and no breakdown was observed during the entire experiment.

4.2. Quantum inefficiency as a function of the ion dose

The inefficiencies obtained from the charge X-profiles of the source can be checked using (2). In this case, one has to make t equals to N_{sec} getting a new expression of the inefficiency expressed by Eq. (3):

$$\mathrm{INEFF}(\mathrm{s}^{-1}, \mathrm{mm}^{-2}) = 1 - \exp(-Q(x) \times P_{\mathrm{ineff}}/e \times N_{\mathrm{site}}). \quad (3)$$

Keeping the above value of $P_{\mathrm{ineff}} = 1 \times 10^{-2}$, the fit is satisfactory for charge $\leqslant 3\,\mathrm{mC/cm}^2$ as shown in Fig. 7. A better result can be obtained with

$$\mathrm{INEFF} = \mathrm{K} \times (1 - \exp -(Q(x)/Q_0)). \quad (4)$$

In the range $\leqslant 3\,\mathrm{mC/cm}^2$, as seen for the irradiation runs in positions 2 and 4, VUV-scanned just after irradiation, the inefficiency varies with the charge with a slope of 15% per $\mathrm{mC/cm}^2$, reflecting the very low occupancy. This value is found significantly larger than the 4% per $\mathrm{mC/cm}^2$ reported recently by Singh [16]. At higher dose, the inefficiency, 40% at $6\,\mathrm{mC/cm}^2$, is less than expected from the linear fit because the increasing number of dead sites renders the irradiation less efficient.

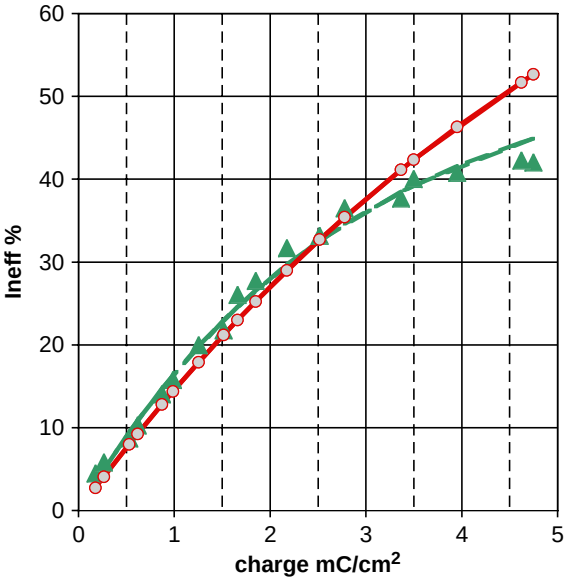

Fig. 7. Triangles: Inefficiency measured along a X-charge profile in position 2, first scan. Fits according to Eqs. (3) and (4), respectively dots and line.

4.3. Experiment lifetime and post-ageing at ALICE–LHC

The ALICE experiment is characterized by a slow event rate, in the range of a few 10^4–10^5 Hz in Pb–Pb and p–p collisions, respectively. However, high multiplicities are expected, reaching for central Pb–Pb collisions 100 particles/m^2 in the HMPID modules located at 5 m from the vertex. The expected charge dose for 10 years operation is estimated to be 0.52 mC/cm^2, shared as 0.45 and 0.07 mC/cm^2 between p–p and Pb–Pb events, respectively [17]. According to the above estimate, a 7.5% QE-drop is expected in the HMPID detector.

During such a long period, a slow degradation of the CsI layer could take place, initiated by a possible reaction with the traces of contaminants (H_2O, other?) in the gases in use (Ar, CH_4). In fact, a long practice has been acquired on that subject since about 30 PCs have been produced and tested over a period of 7 years. Keeping the method of CsI processing unchanged, the QE performance was found reproducible [6]. Several of them were thoroughly tested and irradiated [18]. QE-drops of 1–2% were recorded over a 2 years period with spread or punctual dose irradiations of 0.01 and 0.2 mC/cm^2, respectively. After installation in the STAR experiment at RHIC, a few % QE-drop was observed attributed to the lack of gas flow during the shipment from CERN to BNL (17 h without gas flow). Later on, the PCs were irradiated at low dose, not showing any post ageing effect after 2 years of operation. In conclusion, the QE-drop was not exceeding 4–5% over 4 years.

Therefore, the post-ageing reported in this paper was never observed during the development and exploitation of the PCs. Having presently no sensible explanation, the main difference to be quoted is the much higher dose and rates of irradiation used during the present exposures, possibly triggering a dose rate effect. For instance, the ion neutralization expected from leakage current might generate a contaminated layer disturbing the electronic properties of the CsI surface and slowly evolving with time.

A new series of irradiation is in progress at smaller doses and rates. A first result was obtained at a dose of 0.2 mC/cm^2 deposited in 100 and 300 h. No QE-drop was observed in theVUV-scans performed 2 and 10 days after irradiation.

5. Conclusion

In the framework of the ALICE–HMPID project, large CsI-PCs were irradiated with ionizing charged particles at a dose up to 6 mC/cm^2 and rate of 5 kHz/mm^2. At a dose below 3 mC/cm^2, the resulting QE-drop was found linear with a slope of 15% per mC/cm^2. This result would imply a QE-drop of 7.5% for 10 years operation in p–p and Pb–Pb interaction modes in ALICE at LHC.

The observed rates of inefficiency can be simulated assuming that only a fraction of 1–2% of ions impacts kills the photoemissive sites, the rest of the charge being removed by leakage current. More studies should be done to propose plausible atomic mechanisms initiating the QE-drop.

Acknowledgements

We gratefully acknowledge the excellent technical support of J. van Beelen, Cl. David, P. Ijzermans, M. van Stenis and the contribution of B. Belin. Thanks also to Dr. R. Chechik for her interest in this work.

References

[1] K. Zeitelhack, et al., Nucl. Instr. and Meth. A 433 (1999) 201 (and references therein).
[2] G. Baum, et al., Nucl. Instr. and Meth. A 433 (1999) 201 (and references therein)
S. Dalla Torre, in: Proceedings of the Fifth International Workshop on RICH, Playa del Carmen, 2004.
[3] F. Garibaldi, et al., Nucl. Instr. and Meth. A 502 (2003) 117 (and references therein)
M. Iodice, in: Proceedings of the Fifth International Workshop on RICH, Playa del Carmen, 2004.
[4] Technical Design Report, ALICE-HMPID CERN/LHCC98-19, http://alice-hmpid.web.cern.ch/alice-hmpid/, publications.
A. Gallas Torreira, in: Proceedings of the Fifth International Workshop on RICH, Playa del Carmen, 2004.
[5] I. Tserruya, in: Proceedings of the Fifth International Workshop on RICH, Playa del Carmen, 2004.
[6] H. Hoedlmoser, in: Proceedings of the Fifth International Workshop on RICH, Playa del Carmen, 2004.
[7] H. Rabus, et al., Nucl. Instr. and Meth. A 438 (1999) 94.
[8] F. Piuz, Nucl. Instr. and Meth. A 502 (2003) 76.
[9] F. Piuz, et al., Nucl. Instr. and Meth. A 433 (1999) (178 and 222);
A. Di Mauro, et al., Nucl. Instr. and Meth. A 433 (1999) 190.
[10] J.C. Santiard, et al., in: Proceedings of the Sixth Workshop on Electronics for the LHC, Snowmass, September 1999, p. 431.
[11] H. Hoedlmoser, Characterization of large area CsI photocathodes for the ALICE/HMPID RICH detector, Thesis, Technischen Universitaet Wien, Fakultaet fuer Physik, 2005.
[12] A. Breskin, Nucl. Instr. and Meth. A 371 (1996) 116.
[13] V. Peskov, et al., Nucl. Instr. and Meth. A 515 (2003) 292.
[14] L. Malter, Phys. Rev. 50 (1936) 48;
J. Va'vra, Nucl. Instr. and Meth. A 515 (2003) 1.
[15] J. Va'vra, et al., Nucl. Instr. and Meth. A 387 (1997) 154.
[16] B.K. Singh, et al., Nucl. Instr. and Meth. A 454 (2000) 364.
[17] A. Morsch, et al., ALICE-INT-2002-28, Geneva, CERN.
[18] A. Braem, et al., Nucl. Instr. and Meth. A 515 (2003) 307;
A. Di Mauro, et al., Nucl. Instr. and Meth. A 461 (2001) 584.